

Particle emissions from laboratory combustion of wildland fuels: In situ optical and mass measurements

L.-W. Antony Chen, Hans Moosmüller, W. Patrick Arnott, Judith C. Chow,
and John G. Watson

Division of Atmospheric Sciences, Desert Research Institute, Reno, Nevada, USA

Ronald A. Susott, Ronald E. Babbitt, Cyle E. Wold, Emily N. Lincoln, and Wei Min Hao

Fire Sciences Laboratory, Rocky Mountain Research Station, USDA Forest Service, Missoula, Montana, USA

Received 3 October 2005; revised 16 November 2005; accepted 28 December 2005; published 21 February 2006.

[1] Time-resolved optical properties of smoke particles from the controlled laboratory combustion of mid-latitude wildland fuels were determined for the first time using advanced techniques, including cavity ring-down/cavity enhanced detection (CRD/CED) for light extinction and two-wavelength photoacoustic detection for light absorption. This experiment clearly resolves the dependence of smoke properties on fuel and combustion phase. Intensive flaming combustion during ponderosa pine wood (PPW) burning produces particles with a low single scattering albedo of 0.32 and a specific mass extinction efficiency of $8.9 \text{ m}^2 \text{ g}^{-1}$. Burning white pine needles (WPN) features a prolonged smoldering phase emitting particles that are not light-absorbing and appear much larger in size with an extinction efficiency $\approx 5 \text{ m}^2 \text{ g}^{-1}$. A Mie scattering model was formulated, which estimates the black carbon fraction in the PPW and WPN smoke particles at 66% and 12%, respectively. These observations may refine the current radiative forcing estimates for biomass burning emissions. **Citation:** Chen, L.-W. A., H. Moosmüller, W. P. Arnott, J. C. Chow, J. G. Watson, R. A. Susott, R. E. Babbitt, C. E. Wold, E. N. Lincoln, and W. M. Hao (2006), Particle emissions from laboratory combustion of wildland fuels: In situ optical and mass measurements, *Geophys. Res. Lett.*, 33, L04803, doi:10.1029/2005GL024838.

1. Introduction

[2] Biomass burning, ranging from natural forest fires to different types of anthropogenic combustion, is one of the largest sources of accumulation-mode particles on a global scale [Kasischke and Penner, 2004], strongly affecting the atmospheric radiation budget. During the last decade, there have been extensive studies characterizing biomass-burning particles; however, most key parameters related to particle-radiation interactions, such as particle size, black carbon (BC) content, and mass specific absorption/scattering/extinction ($E_{ap}/E_{sp}/E_{ep}$), are quite inconsistent in the literature. A recent review [Reid *et al.*, 2005a] attributes the inconsistency to: 1) the dynamic nature of fires; 2) variations in smoke aging processes; and 3) differences in measurement techniques. Most of the previous measurements were made during wildland fires [see Reid *et al.*, 2005a] and reflect a mixture of fuels and of flaming and

smoldering combustion phases. Untangling the influence of individual fuels and combustion phases is essential for estimating emissions and impacts from wildland fires because particle characteristics and emission factors vary strongly with these parameters. This untangling can be achieved through laboratory combustion of individual fuels and the time-resolved characterization of combustion products as function of combustion phase.

[3] This paper demonstrates mass and advanced optical measurements for smoke particles emitted from the controlled laboratory combustion of individual wildland fuels. These measurements not only determine E_{ap} , E_{sp} , and E_{ep} but also infer particle size and BC fraction that are most useful for modeling aerosol radiative forcing. This experiment is part of an integrated study conducted at the United States Forest Service Fire Science Laboratory (FSL, Missoula, MT) 19–26 November 2003 with the objectives of characterizing smoke/flame properties, quantifying emission factors, and testing innovative measurement techniques. Emphases have been put on fuels commonly burned in mid-latitude forests.

2. Optical Model

[4] Fresh smoke particles can be described as a two-component system: a light-absorbing BC component and a non-absorbing component containing organic matter (OM) as well as other minor constituents. Extensive microscopic examination of smoke particles [see Reid *et al.*, 2005b and references therein; Chakrabarty *et al.*, 2006] indicate that they are internally mixed for the most part and have a uniform density irrespective of their sizes.

[5] Figure 1 demonstrates how particle diameter and BC fraction might influence the single scattering albedo (ω) and specific mass extinction efficiency ($E_{ep} = E_{sp} + E_{ap}$). It is based on a standard Mie scattering code [Wiscombe, 1980] with Bruggeman mixing rule [Lesins *et al.*, 2002], recommended for a mixture of insoluble particles where the dry aerosol components (i.e., BC and OM) are interspersed. A refractive index \tilde{n} of $1.96 - 0.66i$ at 532 nm is assumed for BC due to its proven effectiveness in several optical-closure analyses [e.g., Fuller *et al.*, 1999; Hand and Kreidenweis, 2002]. The rest of the material is modeled with \tilde{n} of $1.42 - 0.001i$ resulting in a mixture \tilde{n} of $1.45 - 0.03i$ if the BC volume fraction is 5%. The BC and OM mass densities are assumed to be 1.7 g cm^{-3} [Haywood *et al.*, 2003] and 1.2 g cm^{-3} [Turpin and Lim, 2001], respectively. A

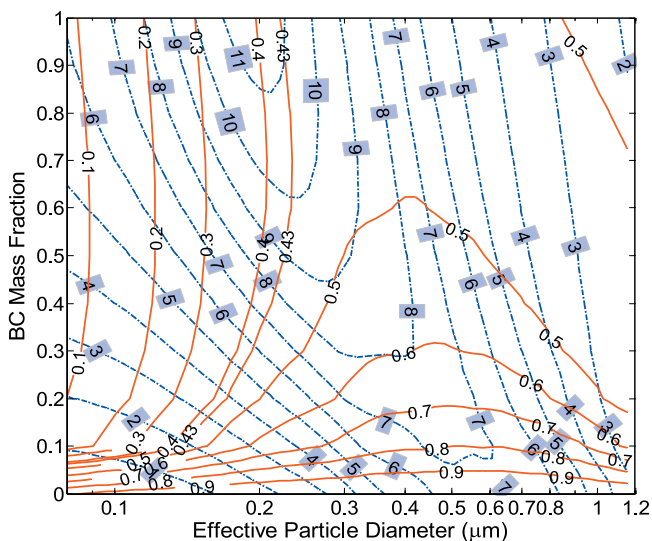


Figure 1. Particle specific mass extinction efficiency (dotted lines; unit- $\text{m}^2 \text{g}^{-1}$) and single scattering albedo (solid lines) as a function of effective particle diameter and mass fraction of BC.

pure BC sphere of $0.14 \mu\text{m}$ diameter would have ω , E_{ep} , and E_{ap} of 0.3, $10 \text{ m}^2 \text{g}^{-1}$, and $7 \text{ m}^2 \text{g}^{-1}$, respectively. E_{ep} of $4.2\text{--}4.7 \text{ m}^2 \text{g}^{-1}$ and ω of $0.82\text{--}0.92$ at mid-visible wavelengths have been reported for six types of wildland fires: fresh/aged grass/savanna, tropical, and temperate/boreal with higher values associated with fresh temperate/boreal fires [Reid *et al.*, 2005a]; effective particle diameters (d_{eff}) of $0.27\text{--}0.33 \mu\text{m}$ can be derived from Figure 1. Small differences between this optical d_{eff} and the measured volume median diameter (VMD, mostly $0.2\text{--}0.3 \mu\text{m}$) [see Reid *et al.*, 2005b] are related to particle size distribution, non-spherical shape of smoke particles, and variability of BC and OM refractive indices and densities. The same ranges of E_{ep} and ω could also yield $d_{eff} = 0.9\text{--}1.1 \mu\text{m}$ (Figure 1) but this size range is seldom observed. From Figure 1, BC may constitute only 5–7% of the particulate emission in these fires.

[6] Particle size and BC fraction referred to hereafter are all retrieved from Figure 1. Chand *et al.* [2005] observe a larger E_{ep} of $6.5\text{--}8.2 \text{ m}^2 \text{g}^{-1}$ and ω of $0.98\text{--}0.99$ during smoldering combustion of Indonesian peat; these are consistent with smoke particles of $0.5\text{--}0.7 \mu\text{m}$ diameter and nearly BC free.

3. Experiment

[7] The combustion facilities at the FSL contain a continuously weighed fuel bed ($80 \times 210 \text{ cm}$) where the burning occurs, and a 1.6 m diameter exhaust stack with a 3.6 m diameter inverted funnel opening 2 m above the fuel bed [Christian *et al.*, 2004]. The stack extends to the ceiling ($\approx 17 \text{ m}$ high) where the sampling platform is located. The fuels were selected to be representative of mid-latitude forest burning [Chakrabarty *et al.*, 2006]. Most fires burned $\approx 250 \text{ g}$ fuel and typically lasted 5–10 minutes, evolving through ignition, flaming, and smoldering phases. Carbon dioxide (CO_2), carbon monoxide (CO), and nitrogen dioxide (NO_2) were monitored by commercial instruments on the sampling platform. The modified combustion efficiency

($\text{MCE} = \text{CO}_2/(\text{CO}_2 + \text{CO})$) [e.g., Yokelson *et al.*, 1996] is used to quantify combustion efficiency.

[8] Total suspended smoke particles were sampled with two photoacoustic instruments (PA) at 532 nm and 1047 nm [Arnott *et al.*, 2000], a hybrid cavity ring-down/enhanced detector (CRD/CED) at 532 nm [Moosmüller *et al.*, 2005], and a tapered element oscillating microbalance (R&P TEOM, Series 1105). A PA measures the light absorption coefficient (σ_{ap}) in the smoke directly at 10-s time resolution with a minimum detection limit (MDL) of $1\text{--}2 \text{ Mm}^{-1}$. The response of PA to light scattering and relative humidity is negligible [Arnott *et al.*, 2003], but NO_2 produced during combustion may interfere with the absorption at 532 nm ($\approx 0.306 \text{ Mm}^{-1}/\text{ppb NO}_2$) [e.g., Arnott *et al.*, 2000]. Spectral dependence of particle light absorption is derived from NO_2 -corrected absorption at the two wavelengths (i.e., $\alpha_{ap} = -\ln[\sigma_{ap,\lambda_1}/\sigma_{ap,\lambda_2}]/\ln[\lambda_1/\lambda_2]$). The TEOM is designed specifically for source sampling of particle mass; 10-s averages were used with a MDL $\approx 50 \mu\text{g m}^{-3}$ and uncertainty $<10\%$ for mass concentration $>500 \mu\text{g m}^{-3}$. The TEOM was calibrated with gravimetric analysis of time-integrated Teflon-filter samples. Combining PA and TEOM has been demonstrated for characterizing diesel exhaust [Moosmüller *et al.*, 2001a, 2001b]. In that study BC and OM masses agree best with those determined by the thermal method when an E_{ap} of $7.36 \text{ m}^2 \text{g}^{-1}$ is assumed for BC.

[9] The extinction (σ_{ep}) measurement based on light attenuation has long been limited by its poor sensitivity. The CRD technique has recently achieved a sensitivity better than 1 Mm^{-1} by implementing a multiple-kilometer optical path in a compact cell with highly reflective mirrors and detecting the energy loss in the cell as a function of time due to aerosol extinction [Moosmüller *et al.*, 2005 and references therein]. The complementary CED technique enhances its dynamic range up to 10^5 . Scattering coefficients (σ_{sp}) were then determined from the difference between CRD/CED and PA measurements. 10-s averaged σ_{ap} , σ_{ep} , and σ_{sp} were divided by 10-s particle mass from TEOM to calculate E_{ap} , E_{ep} , and E_{sp} , respectively. Total and back-hemispheric scattering are usually quantified by integrating nephelometry, but forward scattering detection limited by the truncation angle of a nephelometer [Anderson *et al.*, 1999; Moosmüller and Arnott, 2003] requires empirical corrections based on the scattering Angstrom exponent (α_{sp}). FSL also operated a 3-wavelength nephelometer (TSI 3563) side by side with the PAs and CRD/CED to determine α_{sp} (i.e., $\alpha_{sp} = -\ln[\sigma_{sp,\lambda_1}/\sigma_{sp,\lambda_2}]/\ln[\lambda_1/\lambda_2]$), which is a qualitative measure of the mean particle size. All these data are baseline subtracted to remove contributions from the ambient air.

[10] Reference soot particles were generated by a standard kerosene lamp. At the sampling platform, a mean soot concentration of $51.6 \pm 1.7 \mu\text{g m}^{-3}$ was measured by TEOM during a 55.7-min period where $\text{MCE} > 0.98$. Average particle ω , E_{ap} , E_{sp} , and E_{ep} (532 nm) are 0.43, $6.3 \text{ m}^2 \text{g}^{-1}$, $4.8 \text{ m}^2 \text{g}^{-1}$, and $11.1 \text{ m}^2 \text{g}^{-1}$, respectively. These values are comparable with those by Sheridan *et al.* [2005] and consistent with a $d_{eff} \approx 0.22 \mu\text{m}$. The BC mass fraction (x_{BC}) is more uncertain since both ω and E_{ep} are insensitive to x_{BC} for $0.85 < x_{BC} < 1$. E_{ap} of BC should vary inversely with λ (i.e., $\alpha_{ap} = 1$) for a constant \tilde{n} [e.g.,

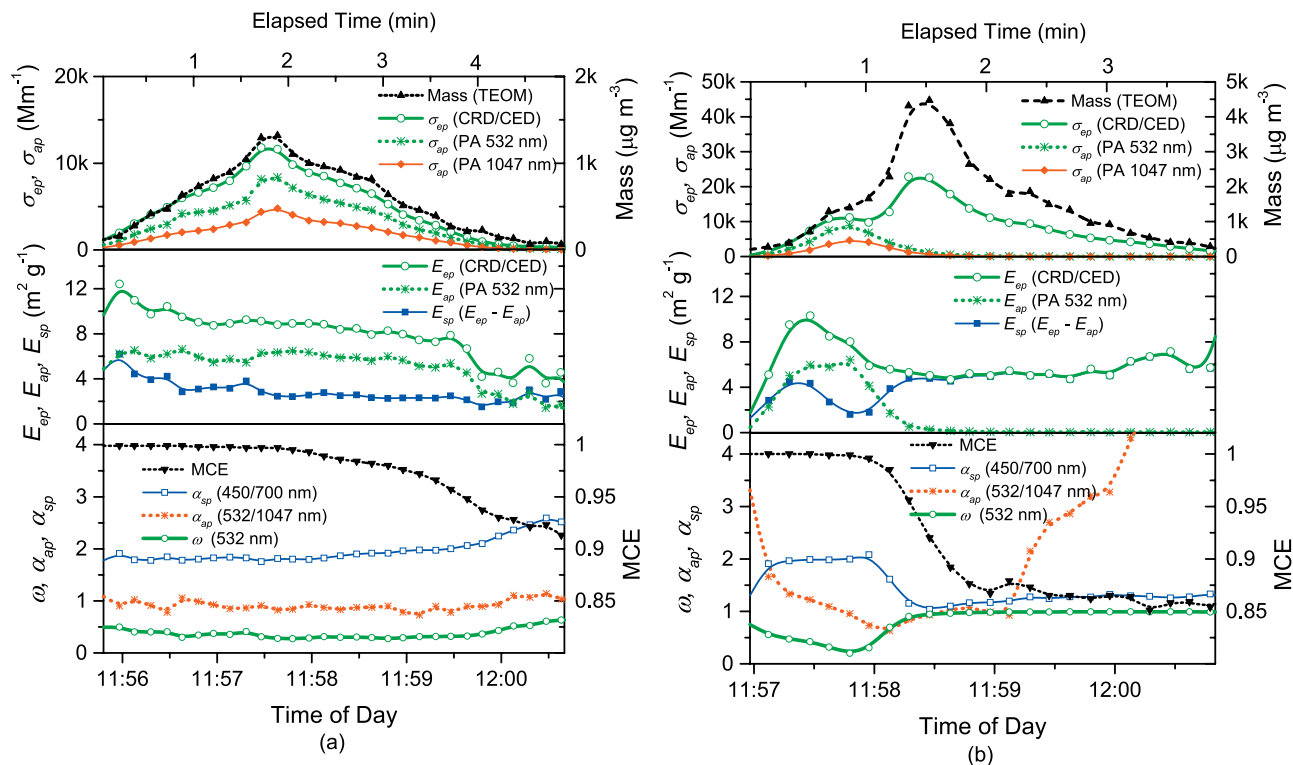


Figure 2. Mass and optical characteristics during laboratory combustion of (a) ponderosa pine wood (PPW) (b) white pine needle (WPN). MCE is the modified combustion efficiency. All symbols indicate 10-s averages and “k” means “ $\times 1000$ ”.

Sheridan *et al.*, 2005]. A measured α_{ap} of 0.90 ± 0.14 (1σ) is not significantly different from 1.

[11] Even after the truncation correction, the nephelometer determines a lower scattering efficiency and therefore a lower albedo ($E_{sp} = 2.2 \text{ m}^2 \text{ g}^{-1}$ at 550 nm; $\omega = 0.26$), based on which a d_{eff} of only $0.14 \mu\text{m}$ would be predicted for the kerosene soot. Mie theory indicates that α_{sp} is more sensitive to particle size for darker (higher x_{BC}) particles; α_{sp} (450/700 nm) changes from 3.5 to 1.4 for pure BC with d_{eff} from 0.14 to $0.22 \mu\text{m}$, while the measured value for kerosene soot is 1.8 ± 0.1 . Moosmüller and Arnott [2003] demonstrate that highly-absorbing particles are more affected by nephelometer truncation than mostly scattering particles. This truncation loss might not be accurately corrected for.

4. Results and Discussions

[12] Dried ponderosa pine wood (PPW) is a common wildland fuel burned in temperate/boreal forest fires. Burning PPW emits highly refractory smoke from a dominant flaming phase. Figure 2a shows the in situ optical (NO_2 -corrected)/mass/gas measurements during a typical PPW burning cycle. Following the simplest definition of smoldering combustion as MCE of < 0.9 [e.g., Yokelson *et al.*, 1996], the PPW combustion does not enter the smoldering phase until the very end of the burning cycle. Pure flaming combustion (MCE > 0.98) during the first 3 minutes contributes $\approx 80\%$ of the total particulate mass emission. The decrease of MCE after this period is associated with a lower combustion temperature after most of the volatile components have been expelled from the PPW and smoldering combustion continues as surface reaction.

[13] An average α_{ap} of 0.89 ± 0.07 during the PPW flaming phase is consistent with that for kerosene soot as well as diesel exhaust particles [Kirchstetter *et al.*, 2004]. The relatively lower ω (on average 0.32) in the PPW smoke can be explained by a smaller particle size ($d_{eff} = 0.15 - 0.17 \mu\text{m}$). E_{ep} and E_{ap} decrease as the combustion process proceeds, and this mostly reflects the reduced BC mass fraction, especially after the flaming phase. By the time MCE drops to 0.92 (≈ 5 min since ignition), ω reaches 0.6. An E_{ep} of $4.5 \text{ m}^2 \text{ g}^{-1}$ then corresponds to a $d_{eff} \approx 0.22 \mu\text{m}$ and $\approx 14\%$ BC. For ambient aerosols α_{sp} seldom increases with particle size, but α_{sp} increases from 1.9 to nearly 2.5 on the transition from the flaming to the smoldering PPW combustion. This occurs as a result of drastic reductions in BC fraction and imaginary refractive index, on the condition of a minor particle size change.

[14] The combustion of white pine needles (WPN; see Figure 2b) contains a short flaming phase (≈ 1 min) followed by an extended smoldering phase (≈ 3 min). Though the same amount of WPN and PPW was burned (250 g), the total particulate mass emission from burning WPN is three times higher. Overall WPN burn much less efficiently than PPW. The ignition of WPN emits relatively white particles ($\omega = 0.75$; $E_{ep} = 2 \text{ m}^2 \text{ g}^{-1}$) that can be modeled with $\approx 5\%$ BC and $d_{eff} = 0.17 \mu\text{m}$. As the combustion proceeds, the BC fraction increases along with the combustion temperature and ω drops to as low as 0.2 implying very small BC particles. The flaming combustion contributes to $\approx 15\%$ of the total particulate emission. E_{ep} is stabilized at $\approx 5 \text{ m}^2 \text{ g}^{-1}$ by the time the burning becomes pure smoldering (MCE = $0.85 - 0.88$) and the smoke is totally white ($\omega > 0.99$). The particle d_{eff} appears to increase to $\approx 0.36 \mu\text{m}$, which is consistent with a lower α_{sp} of ≈ 1.2 . Prior studies [e.g., Reid

et al., 2005a; *Chand et al.*, 2005] have suggested that smoldering combustion may produce larger particles than flaming combustion due to more OM available for condensation on nuclei particles. An E_{ep} of $5 \text{ m}^2 \text{ g}^{-1}$ is at the higher end of estimates by *Reid et al.* [2005a] but significantly lower than those in tropical peat smoke [*Chand et al.*, 2005]. α_{ap} tends to increase with the OM content, averaging at 0.96 and 2.2 for the flaming and smoldering phases, respectively. This has been attributed to significant light absorption by OM in the UV and visible regions $<700 \text{ nm}$ wavelength [*Kirchstetter et al.*, 2004].

[15] Time-averaged σ_{ep} , σ_{ap} , and mass measurements for the WPN burning indicate an overall E_{ep} and ω of $5.6 \text{ m}^2 \text{ g}^{-1}$ and 0.81, respectively. From this, a BC fraction of 7% would be predicted. However, integrating 10-s BC content over the entire combustion yields an overall BC fraction of 12%. BC absorbs light more efficiently as its fraction in the particles decreases [*Martins et al.*, 1998], and this non-uniformity may cause substantial biases for BC retrieval using time-averaged optical measurements. The BC fraction does not vary as much during the PPW burning, and this effect becomes minor. Time-averaged and resolved measurements from the PPW burning yield a BC fraction of 62% and 66%, respectively.

5. Conclusions

[16] Specific mass absorption, scattering, and extinction efficiencies of smoke particles from burning mid-latitude forest fuels are determined with 10-s resolution without some common artifacts, such as the matrix effects of filter-based absorption measurement and truncation losses of scattering measurement by nephelometry. A simple optical model is used to estimate the effective particle size and BC fraction. The dependence of smoke properties on fuel and combustion phase has been clearly resolved. PPW burns more efficiently than WPN, overall generating less and smaller particles. The prolonged smoldering phase during WPN combustion emits larger particles with a higher scattering efficiency. Incorporating these findings into the biomass burning emission inventory may refine aerosol radiative forcing estimates. Absorption varies approximately as $\lambda^{-0.9} - \lambda^{-1}$ for kerosene soot and smoke from flaming combustions; a larger exponent is found for smoke from smoldering combustion with low BC, consistent with a significant absorption by OM in the visible region.

[17] **Acknowledgments.** This work was supported in part by the Joint Venture Agreement 03-JV-11222049-102 between the USDA Forest Service, Rocky Mountain Research Station, Research Work Unit Number 4404 and the DRI. Additional support was provided by the EPA STAR Grant RD-83108601-0. It is a pleasure to acknowledge the help of S. Baker, V. Kovalev, S. Leininger, J. Newton, L. Rinehart, and C. Ryan with the work at the USFS Fire Science Laboratory.

References

Anderson, T. L., D. S. Covert, J. D. Wheeler, J. M. Harris, K. D. Perry, B. E. Trost, D. J. Jaffe, and J. A. Ogren (1999), Aerosol backscatter fraction and single scattering albedo: Measured values and uncertainties at a coastal station in the Pacific Northwest, *J. Geophys. Res.*, *104*, 26,793–26,807.

Arnott, W. P., H. Moosmüller, and J. W. Walker (2000), Nitrogen dioxide and kerosene-flame soot calibration of photoacoustic instruments for measurement of light absorption by aerosols, *Rev. Sci. Instrum.*, *71*, 4545–4552.

Arnott, W. P., H. Moosmüller, P. J. Sheridan, J. A. Ogren, R. Raspet, W. V. Slaton, J. L. Hand, S. M. Kreidenweis, and J. J. L. Collett (2003), Photo-

acoustic and filter-based ambient aerosol light absorption measurements: Instrument comparison and the role of relative humidity, *J. Geophys. Res.*, *108*(D1), 4034, doi:10.1029/2002JD002165.

Chakrabarty, R. K., et al. (2006), Emissions from the laboratory combustion of wildland fuels: Characterization of particle morphology and size, *J. Geophys. Res.*, doi:10.1029/2005JD006659, in press.

Chand, D., O. Schmid, P. Gwaze, R. S. Parmar, G. Helas, K. Zeromskiene, A. Wiedensohler, A. Massling, and M. O. Andreae (2005), Laboratory measurements of smoke optical properties from the burning of Indonesian peat and other types of biomass, *Geophys. Res. Lett.*, *32*, L12819, doi:10.1029/2005GL022678.

Christian, T. J., B. Kleiss, R. J. Yokelson, R. Holzinger, P. J. Crutzen, W. M. Hao, T. Shirai, and D. R. Blake (2004), Comprehensive laboratory measurements of biomass-burning emissions: 2. First intercomparison of open-path FTIR, PTR-MS, and GC-MS/FID/ECD, *J. Geophys. Res.*, *109*, D02311, doi:10.1029/2003JD003874.

Fuller, K. A., W. C. Malm, and S. M. Kreidenweis (1999), Effects of mixing on extinction by carbonaceous particles, *J. Geophys. Res.*, *104*, 15,941–15,954.

Hand, J., and S. Kreidenweis (2002), A new method for retrieving particle refractive index and effective density from aerosol size distribution data, *Aerosol Sci. Technol.*, *36*, 1012–1026.

Haywood, J. M., S. R. Osborne, P. N. Francis, A. Keil, P. Formenti, M. O. Andreae, and P. H. Kaye (2003), The mean physical and optical properties of regional haze dominated by biomass burning aerosol measured from the C-130 aircraft during SAFARI 2000, *J. Geophys. Res.*, *108*(D13), 8473, doi:10.1029/2002JD002226.

Kasischke, E. S., and J. E. Penner (2004), Improving global estimates of atmospheric emissions from biomass burning, *J. Geophys. Res.*, *109*, D14S01, doi:10.1029/2004JD004972.

Kirchstetter, T. W., T. Novakov, and P. V. Hobbs (2004), Evidence that the spectral dependence of light absorption by aerosols is affected by organic carbon, *J. Geophys. Res.*, *109*, D21208, doi:10.1029/2004JD004999.

Lesins, G., P. Chylek, and U. Lohmann (2002), A study of internal and external mixing scenarios and its effect on aerosol optical properties and direct radiative forcing, *J. Geophys. Res.*, *107*(D10), 4094, doi:10.1029/2001JD000973.

Martins, J. V., P. Artaxo, C. Lioussé, J. S. Reid, P. V. Hobbs, and Y. J. Kaufman (1998), Effects of black carbon content, particle size, and mixing on light absorption by aerosols from biomass burning in Brazil, *J. Geophys. Res.*, *103*, 32,041–32,050.

Moosmüller, H., and W. P. Arnott (2003), Angular truncation errors in integrating nephelometry, *Rev. Sci. Instrum.*, *74*, 3492–3501.

Moosmüller, H., W. P. Arnott, C. F. Rogers, J. L. Bowen, J. Gillies, W. R. Pierson, J. F. Collins, T. D. Durbin, and J. M. Norbeck (2001a), Time resolved characterization of diesel particulate emissions. 1. Instruments for particle mass measurements, *Environ. Sci. Technol.*, *35*, 781–787.

Moosmüller, H., W. P. Arnott, C. F. Rogers, J. L. Bowen, J. Gillies, W. R. Pierson, J. F. Collins, T. D. Durbin, and J. M. Norbeck (2001b), Time resolved characterization of diesel particulate emissions. 2. Instruments for elemental and organic carbon measurements, *Environ. Sci. Technol.*, *35*, 1935–1942.

Moosmüller, H., R. Varma, and W. P. Arnott (2005), Cavity ring-down and cavity-enhanced detection techniques for the measurement of aerosol extinction, *Aerosol Sci. Technol.*, *39*, 30–39.

Reid, J. S., T. F. Eck, S. A. Christopher, R. Koppmann, O. Dubovik, D. P. Eleuterio, B. N. Holben, E. A. Reid, and J. Zhang (2005a), A review of biomass burning emissions, part III: Intensive optical properties of biomass burning particles, *Atmos. Chem. Phys.*, *5*, 827–849.

Reid, J. S., R. Koppmann, T. F. Eck, and D. P. Eleuterio (2005b), A review of biomass burning emissions, part II: Intensive physical properties of biomass burning particles, *Atmos. Chem. Phys.*, *5*, 799–825.

Sheridan, P. J., et al. (2005), The Reno aerosol optics study: An evaluation of aerosol absorption measurement methods, *Aerosol Sci. Technol.*, *39*, 1–16.

Turpin, B. J., and H. J. Lim (2001), Species contributions to $\text{PM}_{2.5}$ mass concentrations: Revisiting common assumptions for estimating organic mass, *Aerosol Sci. Technol.*, *35*, 602–610.

Wiscombe, W. J. (1980), Improved Mie scattering algorithms, *Appl. Opt.*, *19*, 1505–1509.

Yokelson, R. J., D. W. T. Griffith, and D. E. Ward (1996), Open-path Fourier transform infrared studies of large-scale laboratory biomass fires, *J. Geophys. Res.*, *101*, 21,067–21,080.

W. P. Arnott, L.-W. A. Chen, J. C. Chow, H. Moosmüller, and J. G. Watson, Division of Atmospheric Sciences, Desert Research Institute, Reno, NV 89512, USA. (lung-wen.chen@dri.edu)

R. E. Babbitt, W. M. Hao, E. N. Lincoln, R. A. Susott, and C. E. Wold, Fire Sciences Laboratory, Rocky Mountain Research Station, USDA Forest Service, Missoula, MT 59807, USA.